Pattern Recognition Letters 2 (1984) 193–197
North-Holland

March 1984

Syntactic recognition of skeletal maturity*

A. PATHAK and S.K. PAL**

Electronics and Communication Sciences Unit, Indian Statistical Institute, Calcutta 700 035, India

R.A. KING

Electrical Engineering Department, Imperial College of Science and Technology, London SW7 2BT, England

Received 28 November 1983

Abstract: A hierarchical three-stage syntactic recognition algorithm using context-free grammars is described for automatic identification of skeletal maturity from X-rays of hand and wrist. The primitives considered are dot, straight line and arcs of three different curvatures (including both senses) in order to describe and interpret the structural development of epiphysis and metaphysis with growth of a child.

Key words: Syntactic pattern recognition, X-ray image.

1. Introduction

The paper describes an algorithm for syntactic recognition of different stages of maturity of bones from X-rays of the hand and wrist. The ultimate aim is to be able to make computer-diagnosis of diseases and effects of malnutrition on the skeletal growth of a child.

During growth of a child, each of the bones of the hand and wrist provides us with an invariant sequence of events which invariably occur in the same order in all individuals and cover the developmental age-span evenly and completely. These sequences therefore give us bases for defining different stages of maturity (age) of the bones. The radius, ulna, metacarpals, phalanges of the hand and wrist provide us with 28 such sequences with events in one or another sequence occurring at almost all stages of development (Tanner et al. (1975)).

* The work was supported by the Medical Research Council, U.K.

** Dr. Pal was on leave with the Electrical Engineering Department, Imperial College of Science and Technology, London SW7, England.

The classifier is based on a hierarchical syntactic approach (Fu (1982)) which accepts contours of the epiphysis and metaphysis as input. Its effectiveness is demonstrated on an X-ray image of radius of a 10–12 year old boy when dot, line and arcs of three different curvature are considered as primitives.

2. Different stages of maturity

Fig. 1 shows eight different stages of skeletal maturity of radius of hand and wrist. This is con-

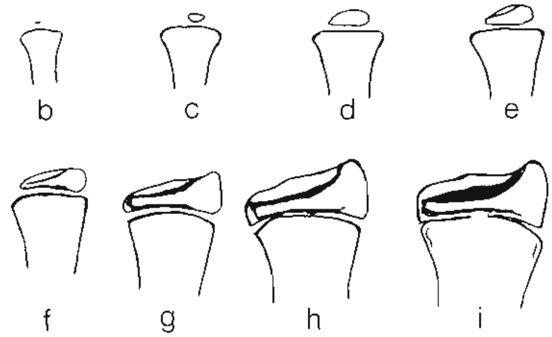

Fig. 1. Different stages of skeletal maturity of radius.

sidered as a typical illustration since radius contributes mostly in determining maturity score (Tanner et al. (1975)). Its structural development with growth of a child is explained below.

In the beginning, the epiphysis is totally absent (Stage A). It gradually appears above the metaphysis as a single (or, rarely, as multiple) deposit(s) of calcium with irregular outline (Stage B). After that, it gradually assumes a well-defined oval shape as seen in the radiograph (Stage C). It continues to grow in size but becomes slightly tapering at its medical end, being more rounded at the lateral end (Stage D). In Stage E, its shape is more or less the same though it becomes larger and a thickened white line representing the edge of the palmar surface, appears within it at the distal border. In the next stage (F), the palmar surface of the proximal border also develops and becomes visible as a thickened white line at the proximal edge of the epiphysis. At stage (G) the palmar surface of the medial border also becomes apparent as a white line so that the three visible palmar surfaces combine to appear as a single continuous, thickened U-shaped contour. The epiphysis continues to grow larger and by stage (H), it caps the metaphysis almost entirely (at one end or both). The styloid process is also much developed. At the last stage (I), fusion of the epiphysis and the metaphysis begins.

The features of the structural development of the radius therefore include the contour, shape and orientation of the metaphysis and epiphysis including palmar and dorsal surfaces as appeared on the epiphysis and metaphysis with the growth and styloid process.

A similar sequence of stages of structural development is also found to be maintained in the other bones, namely, ulna, metacarpals and phalanges.

3. Classification algorithm

We have used the following alphabet of 8 primitives:

$$V_T = \{a, b, c, d, \bar{b}, \bar{c}, \bar{d}, e\}$$

where

a = line segment of unit length,
b = gentle clockwise curve,
c = fair clockwise curve,
d = sharp clockwise curve,
e = dot.

$\bar{b}$, $\bar{c}$, $\bar{d}$ are the anticlockwise versions of b, c, d respectively.

The method used for constructing the grammars is a heuristic one (Fu (1982)) which involves enumerating for each class of the set of possible patterns first. Then, in terms of the available terminals and predicates, we frame the production rules for each string and then pool all of them together and reduce them by the heuristic rules given to get the set of production rules for the entire class.

The procedure for assigning ratings is hierarchical in nature and involves three stages as shown in Fig. 2.

Step 1 (primary classification). This classification is done with the help of four context-free grammars

$$G_i = \{V_{N_i}, V_T, P_i, S\}, \quad i = 2, \ldots, 5,$$

such that if an unknown string (X) representing

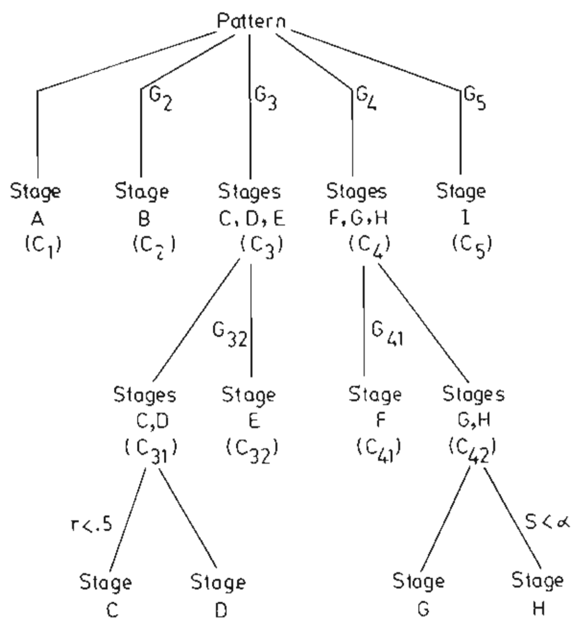

Fig. 2. Three stage hierarchical classification scheme.

the contour of epiphysis

$$X \in L(G_i), \quad i=2,\dots,5,$$

then it is classified into class C_i, the classes C_i, $i=2,\dots,5$, being defined as follows:

$$C_2=\{\text{Stage B}\}, \qquad C_3=\{\text{Stages C, D, E}\},$$

$$C_4=\{\text{Stages F, G, H}\}, \qquad C_5=\{\text{Stage I}\}.$$

Otherwise X is classified into $C_1=\{\text{Stage A}\}$ where the epiphysis is totally absent. $L(G_i)$ denotes the language generated by the grammar G_i.

The reasons for adopting this particular form of clustering of the stages A–I are rather self-evident. For example, each of stages A and B is unique in itself and hence each is put in a separate class.

For assigning the stages C, D, E into the same class C_3, we were guided by the fact that in each of these stages X tends to have the general form

CC—CC

CC—SL—CC—SL

which is distinct from the general forms of X for stages, F, G, H comprising C_4, viz.

CC—SL—CC—CC—SL

CC—CC—SL—CC—CC—SL

CC—CC—SL—CC—SL—CC—SL

where CC denotes a clockwise curve (fair or sharp) and SL denotes any straight line segment (which may include some gentle curves).

Obviously there is a possibility that C_3 and C_4 may overlap, mainly because of the similarity in stages E and F in respect of X. We have made provisions at steps 2.1 and 2.2 for minimizing the error resulting from this.

Again, stage I is put in a separate class (C_5) by itself, because it is unique in the sense that instead of getting separate images of the epiphysis and the metaphysis, we get one continuous contour of the image structure which results from the fusion of the two.

Table 1 explains the possible strings and the corresponding production rules for the different classes.

Step 2. We come here for further classification in case the unknown string $X \in L(G_3)$ or $L(G_4)$.

For this purpose we obtain a string description (Y) of the contour of the interior (palmar and dorsal surface) of the epiphysis.

Step 2.1. If $X \in L(G_3)$ and $Y \in L(G_{32})$, we classify the pattern into C_{32} (stage E). In constructing the production rules P_{32} (Table 1) corresponding to the grammar G_{32} we are guided by the fact that at stage E (unlike in stages C, D) the image of the interior of epiphysis becomes non-empty for the first time due to the appearance of a thickened line (as explained in Section 2).

If $X \in L(G_3)$ but $Y \notin L(G_{32})$, then there are two possibilities, namely the pattern may be from C_{31} (stages C, D) or from C_{41} (stage F). To check the correct one we go to step 2.3(a).

Step 2.2 If $X \in L(G_4)$ and $Y \in L(G_{41})$ we classify the pattern into C_{41} (stage F). The production rules for G_{41} are shown in Table 1.

If $X \in L(G_4)$ but $Y \notin L(G_{41})$ then there are two possibilities, namely the pattern may be from C_{42} (stage G, H) or from C_{32} (stage E). To check the correct one we go to step 2.3(b).

Step 2.3(a). If $X \in L(G_3)$ but $Y \notin L(G_{32})$ we check if $Y \in L(G_{41})$. If so, we classify the pattern into C_{41}. If not, we classify it into C_{31} and go to step 3.1.

Step 2.3(b). If $X \in L(G_4)$ but $Y \notin L(G_{41})$ we check if $Y \in L(G_{32})$. If so, we classify the pattern into C_{32}. Otherwise, we classify it into C_{42} and go to step 3.2.

Step 3.1. If the unknown pattern is classified into C_{31}, the maximum diameter (D_E) of the epiphysis as well as the width (W_M) of the metaphysis is determined. There are numerous algorithms available in the texts for this purpose (Fu (1982)).

If $r=D_E/W_M \leq 0.5$, assign the pattern to stage C. Otherwise, decide stage D.

Step 3.2. If the unknown pattern is classified into C_{42}, we determine the slopes S_E and S_M (at the medial end) of the proximal edge of the epiphysis and the distal edge of the metaphysis.

If $S=|S_E-S_M|$ < some pre-determined α, suit-

Table 1
Production rules for the grammars

Class	Possible strings	Production rules for grammar for the class				
C_2	X = e	P_2	S → e			
C_3	X = cc, dd, cd, dc	P_3	S → AA	A → BC	A → c	
	$a^m da^n d$, $a^m ca^n d$, $a^m ba^n d$,		A → d	B → aB	B → a	
	$a^m ba^n c$, $a^m ca^n c$, $a^m ba^n b$		C → b	C → c	C → d	
	where m, n are positive integers					
C_4	X = $Pda^q dQ$, $Pca^q cQ$, $Pba^q bQ$	P_4	S → AB	A → CDC	A → CFC	B → D
	$Pda^q cQ$, $Pda^q bQ$, $Pca^q bQ$		B → c	B → d	C → aC	
	where $P = a^r$ or $a^r ba^s$,		C → a	D — BB	D → EE	
	$Q = a^t R$, R = b, c or d		D → BE	D → BCB	D → ECE	
	and q(≥0), r, s, t(>0) are integers		D → BCE	F → bCD	E → b	
C_5	X = L $\bar{M}$ M L M L $\bar{M}$ L	P_5	S → ABA	A → aA	A → a	
	where M = b or c or d		A → C	A → AC	A → CA	
	$\bar{M}$ = anticlockwise version of M		C → CC	C → b	C → $\bar{b}$	
	L = a^x, $a^x ba^y ba^z$,		B → DAE	D → FG	E → GAF	
	$a^x ba^y \bar{b}a^z$, $a^x \bar{b}a^y ba^z$,		F → $\bar{b}$	F → $\bar{c}$	F → $\bar{d}$	
	$a^x \bar{b}a^y \bar{b}a^z$		G → b	C → c	G → d	
	where x, z(>0) and y(≥0) are integers					
C_{32}	Y = LdLd, LdLc, LcLd,	P_{32}	S → AA	A → BC	B → aB	
	LcLc,		B → a	B → BD	B → DB	
	where L is as above		B → D	D → DD	D → b	
			D → $\bar{b}$	C → c	C → d	
C_{41}	Y = L M L $\bar{M}$ L M L M L^+ $\bar{M}$ L^+ M	P_{41}	S → AB	A → CDC	B → EDF	
	where L, N, $\bar{M}$ are as above		C → GIG	D → $\bar{b}$	D → $\bar{c}$	D → $\bar{d}$
	$L^+ = a^x$, x > 0		E → IJ	E → I	F → JI	F → I
			G → aG	G → a	G → HG	G → GH
			G → H	H → HH	H → b	H → $\bar{b}$
			I → b	I → c	I → d	J → a
			J → aJ			

ably small, then the pattern is assigned to stage H.

Otherwise, it is assigned to stage G.

In practice S_E and S_M are reflected by their degree of arcness μ_{arc} (as explained in the Section 4) at the medial end.

Some practical considerations

The classification algorithm as described before has been developed on the basis of the actual edge detected radiographs for the different stages. As far as possible, the minor variations in pattern that are quite likely to occur have been accounted for in the grammars.

However in practice, due to the limitations of the pre-processing (digitisation, thresholding, enhancement and contour extraction) algorithms it is quite likely that we may encounter situations in which the above algorithm will need some modification for machine identification of different stages. For instance, in the cases of C_3 and C_4 (though it is very unlikely for C_3), we may obtain an edge-detected image in which the contours representing the epiphysis and the metaphysis are partly joined. In such a case, we skip the method of primary classification in step 1 and proceed from step 2 for final classification.

4. Implementation and results

As seen in Section 3, the classification algorithm needs as input an X-ray pattern in the form of a string comprising the primitives (terminals a, b, c,

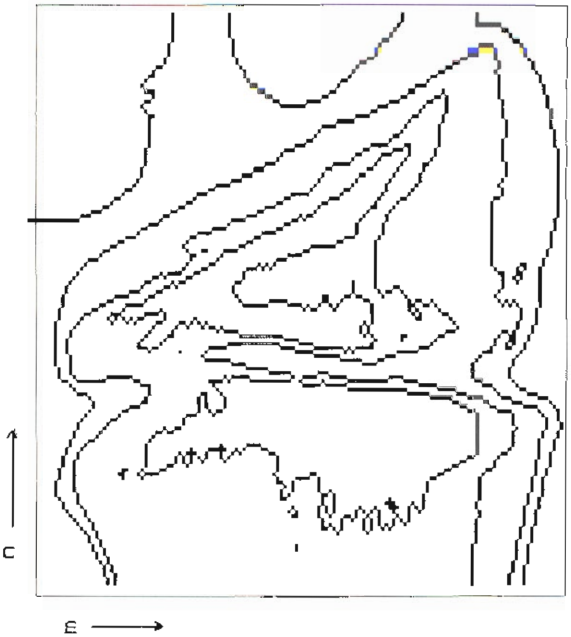

Fig. 3. Input image.

d). These primitives are again extracted from the contours of the bones of hand and wrist.

Fig. 3 shows an edge-detected version of an 128×145 dimensional radius of a 10–12 year old boy (Pal and King (1983)). These contours are extracted using a contrast intensification operator along with S and π membership functions. The computer-based description of the contours (with 90° clockwise rotation) after octal code representation, smoothing to remove the spurious wiggles and segmentation, is explained below (Pal et al. (1983)):

(i) Starting point of contour (22,1); end of contour (129,1). Description of the contour is as follows:

$$L_3\, A_{0.465}\, L_2\, \bar{A}_{0.541}\, L\, A_{0.272}\, L\, A_{0.272}\, L_{15}\, A_{0.533}\, L_7\, A_{0.272}\, L_3\, \bar{A}_{0.465}\, L_2\, A_{0.541}\, \bar{A}_{0.272}\, L\, A_{0.272}$$

(ii) Starting point of contour (24,1); end of contour (119,1). Description of the contour is as follows:

$$\bar{A}_{0.272}\, L_2\, A_{0.377}\, L_3\, \bar{A}_{0.644}\, L_2\, A_{0.488}\, L_{12}\, A_{0.757}\, L_4\, \bar{A}_{0.348}\, L_4\, A_{0.644}\, \bar{A}_{0.272}\, A_{0.272}\, L_8\, \bar{A}_{0.702}\, L_3\, A_{0.816}\, L_2\, \bar{A}_{0.644}\, A_{0.541}\, L_4\, \bar{A}_{0.765}\, L_3\, A_{0.465}\, L\, \bar{A}_{0.541}\, \bar{A}_{0.645}\, \bar{A}_{0.587}\, A_{0.559}\, \bar{A}_{0.816}\, A_{0.707}\, A_{0.272}\, \bar{A}_{0.47}\, L_3\, \bar{A}_{0.429}\, L_5\, \bar{A}_{0.816}\, L_6\, A_{0.272}\, L\, A_{0.317}\, L_2\, \bar{A}_{0.272}\, L_2$$

(iii) Starting point of contour (22,64); the contour is closed. Description of the contour is as follows:

$$L_{11}\, A_{0.86}\, L_4\, A_{0.272}\, L\, \bar{A}_{0.662}\, L_4\, A_{0.598}\, L_7\, \bar{A}_{0.272}\, A_{0.765}\, \bar{A}_{0.816}\, \bar{A}_{0.272}\, L\, A_{0.765}$$

where L, A and Ā denote the 'straight line', 'clockwise arc' and 'anti-clockwise arc' respectively. Suffices of L and A represent the number of line units and the degree of 'arcness' (μ_{arc}) of the arc A respectively. Since we are interested only with the epiphysis and metaphysis, other contours of the image (Fig. 3) are not considered.

From this image pattern we find that the contours representing the epiphysis and the metaphysis are partly joined. So we proceed directly from Step 2 of the algorithm. Here we have the string corresponding to the palmar and dorsal surface

$$Y = a^{11}\ d\ a^4\ b\ a\ \bar{d}\ a^4\ c\ a^7\ \bar{b}\ d\ \bar{d}\ \bar{b}\ a\ d$$

where $0.2 \le \mu_{arc} \le 0.4$, $0.4 < \mu_{arc} \le 0.6$ and $0.6 < \mu_{arc} \le 1$ are considered to be primitives b, c and d respectively. On parsing, it is found that $y \in L(C_{41})$. Thus we assign this X-ray image pattern to the stage F.

References

Tanner, J.M., R.H. Whitehouse, W.A. Marshall, M.J.R. Healy and H. Goldstein (1975). *Assessment of Skeletal Maturity and Prediction of Adult Height (TW2 Method).* Academic Press, New York.

Fu, K.S. (1982). *Syntactic Pattern Recognition and Applications*, Prentice-Hall, Englewood Cliffs, NJ.

Pal, S.K. and R.A. King (1983). On edge detection of X-ray images using fuzzy sets. *IEEE Trans. Pattern Anal. Machine Intelligence* 5, 69–77.

Pal. S.K., R.A. King and A. Hashim (1983). Image description and primitive extraction using fuzzy sets. *IEEE Trans. Systems Man Cybernet.* 13, 94–100.